Journal of Power Sources 248 (2014) 582–587

Contents lists available at ScienceDirect

Journal of Power Sources

journal homepage: www.elsevier.com/locate/jpowsour

Short communication

Aqueous lithium ion batteries on paper substrates

Ke Sun [a], Diego A. Juarez [b], Huang Huang [a], Euiyeon Jung [a], Shen J. Dillon [a,*]

[a] Department of Materials Science and Engineering, University of Illinois Urbana-Champaign, IL 61801, United States
[b] Department of Mechanical Engineering, University of Idaho, Moscow, ID 83843, United States

HIGHLIGHTS

- Conductive carbon-coated TiP_2O_7 powder was synthesized by a solid state reaction.
- Carbon nanotube solution processing was used to convert paper into conductive substrates.
- $LiMn_2O_4$ and TiP_2O_7 slurries were coated onto conductive paper substrates as cathode and anode.
- Electrodes were assembled and tested in aqueous electrolyte.
- The battery showed excellent rate capability and cycle life.

ARTICLE INFO

Article history:
Received 4 June 2013
Received in revised form
23 September 2013
Accepted 26 September 2013
Available online 7 October 2013

Keywords:
Carbon coated TiP_2O_7
$LiMn_2O_4$
Conductive paper
Aqueous lithium ion battery

ABSTRACT

Aqueous paper batteries were fabricated and demonstrated based on $LiMn_2O_4$ and carbon coated TiP_2O_7. Carbon nanotubes conformally coated commercial paper, which served as current collectors. Anode and cathode slurries penetrated these conductive substrates well. Aqueous paper batteries were tested electrochemically, exhibiting excellent rate capability and reasonable cycling life. TiP_2O_7 dissolution accounts for the observed capacity fade.

1. Introduction

For millennia [1], paper has remained a key human technology applied in a variety of applications ranging from substrates for printed language and aircraft material to analog recording media and data transmission. Recently, researchers have revisited paper as a candidate substrate for electronic devices. Paper's attractive qualities extend beyond its low-cost and environmental friendly nature to its ability to absorb and bind different inks as a result of its hierarchical porous and fibrous structures and its surface chemistry. A wide variety of electronic and biomedical devices have been demonstrated on paper substrates, including organic photodiodes [2], organic thin-film transistors [3], thermochromic displays [4] and disposable microfluidic and diagnostic devices [5]. Low cost patterned devices may be fabricated simply based on ink-jet or e-jet printing. Ideally, high power and high energy density storage media would be integrated on paper substrates in ambient conditions to enable new low cost devices. The surface roughness and porous structure of paper endow it with large surface area, which is desirable in electrochemical storage applications, such as supercapacitors and Li-ion batteries. Hu and Cui demonstrated that paper can serve as light-weight and flexible current collectors for supercapacitors and non-aqueous lithium ion batteries when coated by single wall carbon nanotubes (SWCNT) [6]. They have shown that these paper-based electrochemical power sources possess similar or even superior rate performance and cycling stability when compared with their traditional counterparts, which are deposited on metallic current collectors. They also outperform polymer substrates utilized for flexible energy storage applications in terms of adhesion of the electrode materials.

Replacement of metal current collectors with paper current collectors in lithium ion batteries would reduce their cost and weight. Paper batteries also hold the promise of powering next generation flexible electronics, but effective battery packaging

* Corresponding author. Department of Materials Science and Engineering, 1304 W. Green St., Urbana, IL 61801, United States. Tel.: +1 217 244 5622.
E-mail address: sdillon@illinois.edu (S.J. Dillon).

0378-7753/$ – see front matter © 2013 Elsevier B.V. All rights reserved.
http://dx.doi.org/10.1016/j.jpowsour.2013.09.114

strategies remain to be developed [7]. However, these initial trials utilize non-aqueous electrolyte, which is highly flammable and can cause safety hazards if used improperly (e.g. overcharging or short-circuiting). Inherently flammable paper current collectors might exacerbate the hazard associated with catastrophic failure. A possible approach to circumvent this problem is to use an aqueous electrolyte, which adopts a "rocking-chair" concept similar to the organic lithium-ion battery [8]. Aqueous chemistry lithium ion batteries have been successfully demonstrated primarily using NASICON type compounds as anode materials and layered transitional metal oxides as cathode materials [9,10]. Aqueous electrolytes also typically offer cost savings, faster diffusion kinetics, and simplified ambient assembly. Aqueous Li-ion based systems are ideal for fabrication in ambient environments, because the electrode materials and electrolyte are stable in air and relatively non-toxic. These benefits make aqueous Li-ion paper batteries an ideal technology for simple low cost energy storage and enable new device design opportunities for engineers and enthusiasts. For example, the technology also generates new opportunities for pen on paper power sources to complement pen on paper electronics [11] and expand the range of devices that can be deterministically assembled by hand in the field.

This work demonstrates paper based Li-ion batteries functioning in aqueous electrolyte. Commercial $LiMn_2O_4$ cathode materials and synthesized carbon coated TiP_2O_7 anode materials will serve as electrodes on SWCNT coated paper substrates. We anticipate such batteries should perform well in terms of energy and power density, with respect to their aqueous secondary battery counterparts. While the approach is a combination of two existing technologies, paper batteries and aqueous Li-ion batteries, it is not trivial to assume that this technology will function effectively. The structure of paper is sensitive to water infiltration, which will affect the electrodes coated on this substrate. Additionally, the interactions between water and the relatively hydrophobic conductive carbons, SWCNT, and polymers could influence overall stability of the structure.

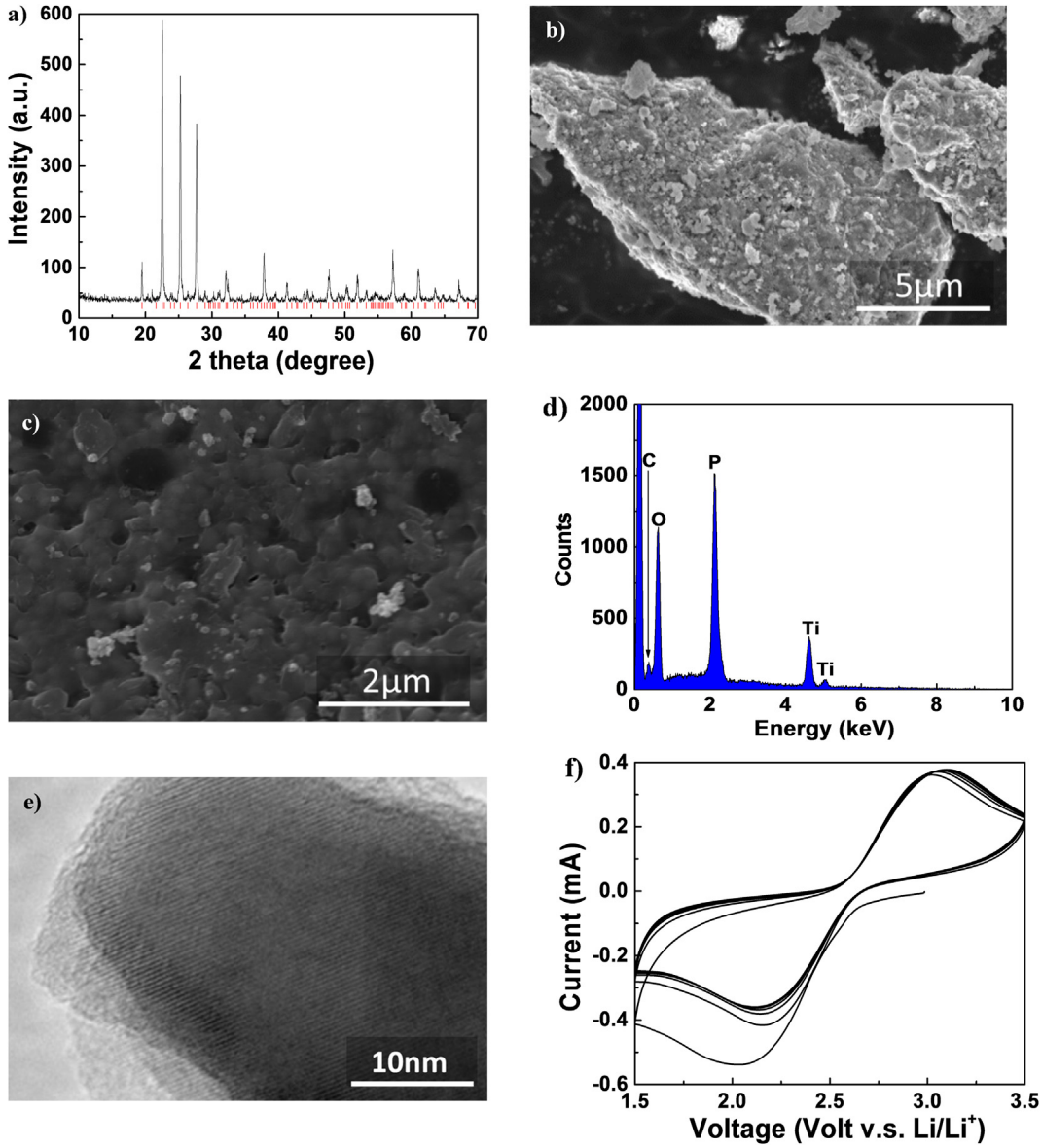

Fig. 1. (a) XRD pattern of as synthesized carbon coated TiP_2O_7. (b) and (c) SEM images of a TiP_2O_7 particle at different magnifications. (d) EDX spectrum of the area shown in (b). (e) TEM image of a single TiP_2O_7 particle. (f) Cyclic voltammetry profile of carbon coated TiP_2O_7 with lithium metal as both counter and reference electrodes, scanning rate: 5 mV s^{-1}.

2. Experimental

2.1. Synthesis and characterization of carbon coated TiP_2O_7 powder

In a typical synthesis, 14.84 g anatase TiO_2 (Alfa Aesar 99.9%), 5.16 g $NH_4H_2PO_4$ (Alfa Aesar 99.99%), and 1.43 g hydroxyethylcellulose (Sigma–Aldrich 99.9%) were mixed and ball milled with alumina media for 24 h to produce a homogeneous precursor. This white precursor powder was annealed in a tube furnace at 700 °C for 30 min. During annealing, argon flowed through a toluene bubbler at room temperature and then through the tube furnace. After annealing, a coarse dark gray product was hand milled in a mortar and pestle. In the reaction, TiO_2 and $NH_4H_2PO_4$ decomposed and reacted to form TiP_2O_7. At the same time, hydroxyethylcellulose was pyrolyzed into glassy carbon. The presence of toluene vapor ensured continuous carbon coating of the TiP_2O_7. The resulting dark gray powder is characteristic of the elemental carbon. The powder was characterized via X-Ray diffraction (XRD, Siemens-Bruker 5000), scanning electron microscopy (SEM, Hitachi S-4700), and transmission electron microscopy (TEM, JEOL 2100).

2.2. Paper electrodes processing

The conductive paper substrates were fabricated according to Ref. [6]. To form a SWCNT ink, SWCNTs (Nano lab) and sodium dodecylbenzenesulfonate (Sigma–Aldrich) were dispersed in deionized water. Their concentrations were 10 and 1 mg mL^{-1}, respectively. After bath sonication for 5 min, the SWCNT dispersion was probe-sonicated for 30 min at 200 W within an ice bath. This process resulted in a reasonably uniform ink. A doctor blade was used to coat the SWCNT ink onto Xerox (Boise) paper. The sheet resistance of conductive paper was measured by using the four-point probe technique (EDTM).

Cathode and anode slurries were made by mixing $LiMn_2O_4$ (Sigma–Aldrich) or TiP_2O_7, Super P carbon (TIMCAL) and PVDF-HFP copolymer (Arkema Kynar Flex® 2801) with a volumetric ratio of 85:10:5 in 1-methyl-2-pyrrolidinone (Sigma–Aldrich) solvent. The slurry was then casted onto the conductive paper substrates with a doctor blade, dried under an infrared lamp and then placed in a vacuum oven to yield the final electrodes. Scanning electron microscopy was applied to characterize the microstructure of the sample during each step of the process.

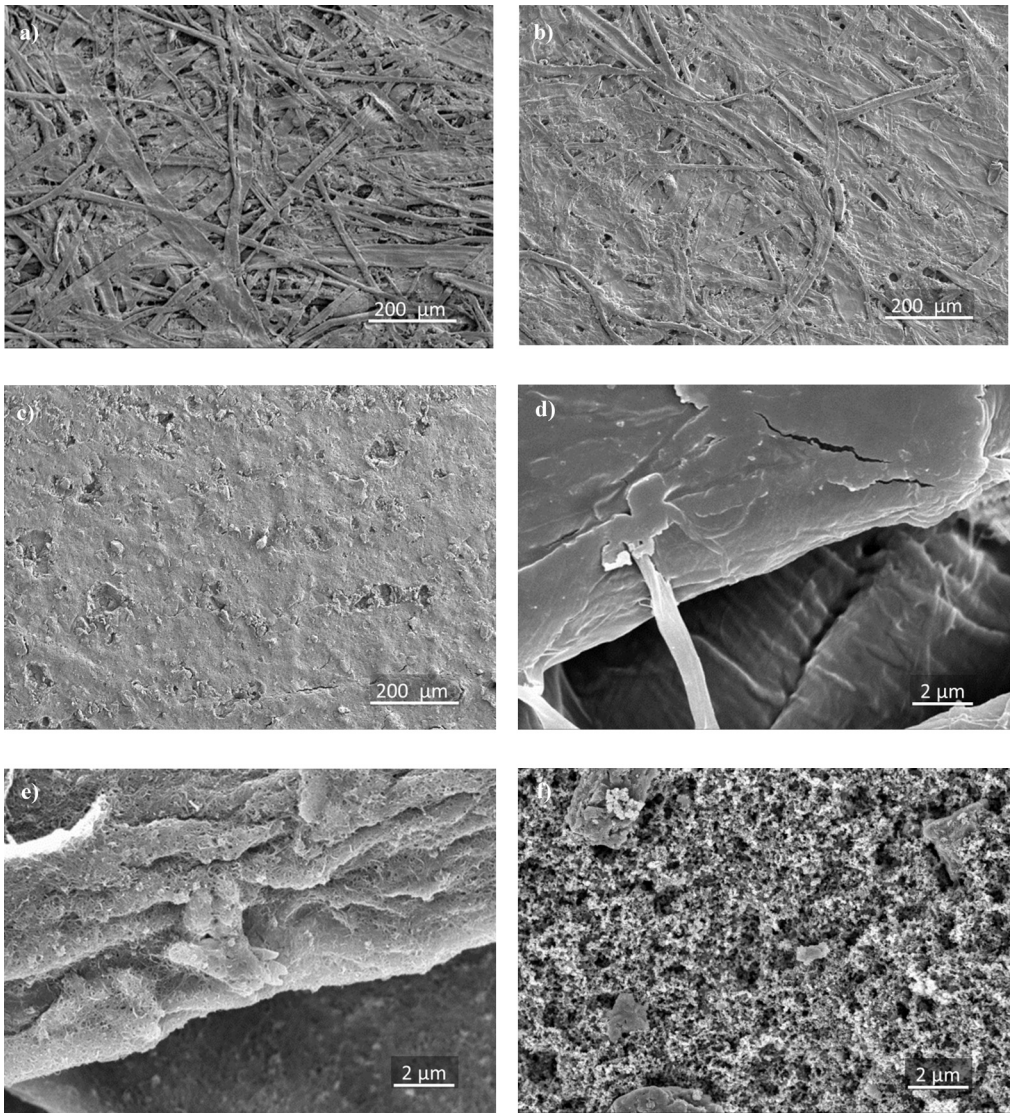

Fig. 2. (a)–(c) Low magnification SEM images of Xerox paper before CNT coating, after CNT coating and after both CNT coating and electrode slurry deposition. (d)–(f) High magnification SEM images of Xerox paper before CNT coating, after CNT coating and after both CNT coating and electrode slurry deposition.

2.3. Electrochemical test

Baseline electrochemical characterization of TiP_2O_7 versus Li was performed in nonaqueous electrolyte, Swagelok-type cells were assembled in an argon-filled glove box. These cells were comprised of a Li metal disc as both the reference and counter electrode, a separator saturated with a 1 M $LiPF_6$ solution in ethylene carbonate (EC) dimethyl carbonate (DMC) (1:1 in weight) as the electrolyte, and the TiP_2O_7 paper electrode as the working electrode. In order to test the performance of the aqueous paper battery, a pouch cell was assembled in ambient condition using $LiMn_2O_4$ as the cathode, TiP_2O_7 as the anode, and a piece of filter paper saturated with 5 M $LiNO_3$ aqueous solution as separator. Both cells were tested by cyclic voltammetry, and galvanostatic charge and discharge using a potentiostat/galvanostat (SP200, Biologic Co, Claix, France).

3. Results and discussion

3.1. Characterization of carbon coated-TiP_2O_7 particles

A powder diffraction pattern of as-synthesized carbon coated TiP_2O_7 is shown in Fig. 1a. The sharp and intense peaks in the pattern indicate the highly crystalline nature of the material. The pattern can be indexed according to the cubic 3 × 3 × 3 super structured TiP_2O_7 with Pa3 space group. The crystallite size calculated using the Scherrer equation is 63(±5) nm. The TiP_2O_7 phase accounts for all of the diffraction peaks in the pattern and no other crystalline phase is identified. The pyrolyzed carbon should be either amorphous or at concentrations insufficient to produce discernible peaks.

The primary particle size of TiP_2O_7 is on the order of tens of μm s with a broad size distribution as observed by SEM in Fig. 1b. However, higher magnification (Fig. 1c) reveals that the larger particles are porous and composed of smaller crystallites. They also have a broad size distribution varying between about 0.1 and 2 μm. This hieratical and porous structure should be advantageous as the high surface area will enhance the rate capability of the electrode particles without significantly compromising the volumetric energy density, which commonly results from inefficient packing of nanoparticles [12]. Energy dispersive x-ray spectroscopy (Fig. 1d) reveals the presence of Ti, O, P, and C. TEM images (Fig. 1e) confirm the presence of a thin amorphous carbon film coating the TiP_2O_7 particles. This film resembles carbon films reported elsewhere in the literature [13,14]. On the basis of the SEM images and EDS it is inferred that this thin coating material is carbon based.

Fig. 1f depicts the results of cyclic voltammetry performed on the carbon coated TiP_2O_7 cycled against lithium in nonaqueous electrolyte. At a scanning rate of 5 mV s^{-1}, anodic and cathodic peaks occur near 3.1 V and 2.1 V, respectively. The equilibrium potential of the reaction between TiP_2O_7 and lithium exists at ~2.6 V [15]. The reduction in cathodic peak current after the first discharge results from irreversible intercalation of approximately 0.2 units of Li, which is commonly observed for TiP_2O_7 [15]. Overall, the reversibility and rate capability of the TiP_2O_7 are reasonable during the first few cycles as shown in the plot.

3.2. Characterization and electrochemical testing of the paper based electrodes and batteries

The use of paper as current collectors for aqueous batteries requires SWCNT coating to enhance the electrical conductivity. The conductive carbon filler in the electrode slurry itself only guarantees through thickness electronic percolation and does not provide significant in-plane electronic percolation. SEM images of paper substrates before SWCNT ink coating, after SWCNT ink coating, and after subsequent electrode slurry coating are shown in Fig. 2. The lower magnification images (Fig. 2a–c), demonstrate the progressive

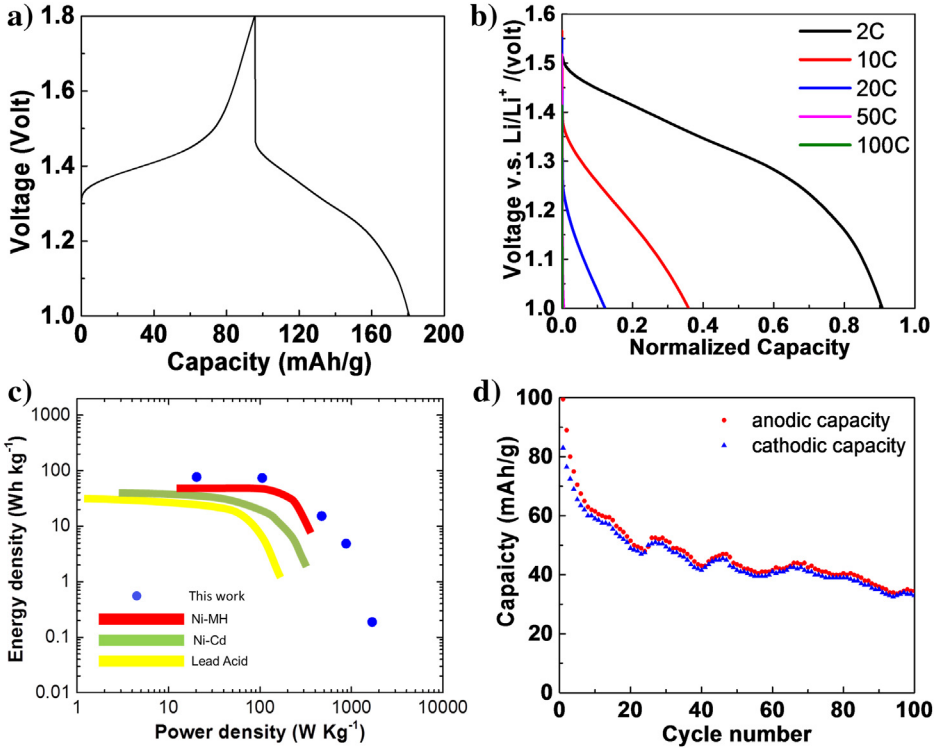

Fig. 3. (a) A representative charge–discharge curve of $LiMn_2O_4$–TiP_2O_7 aqueous paper battery. (b) Discharge curves of the battery at different current densities. (c) Comparison of the rate capability of a $LiMn_2O_4$–TiP_2O_7 aqueous paper battery with other aqueous battery systems. (d) Cycling performance of the battery for 100 cycles.

filling of porosity and the gradual elimination of the fiber texture at the surface. The higher magnification images (Fig. 2d–f), reveal how the fibers are first covered by sub 100 nm thick nanofibrils, which should be CNT coming from the coating process, and subsequently by a layer of TiP_2O_7 particles. These images show the conformal nature of the SWCNT ink coating, which does not destroy the microscale porosity of the paper. The electrode slurry subsequently fills these pores and fills the entire electrode more efficiently.

In order to test the efficacy of the SWCNT coating in enhancing electronic conductivity, the sheet resistance was measured for the 3 paper samples shown in Fig. 2. The stock paper is completely resistive and no measured value is obtained. After SWCNT coating the resistance reduced to 120 Ω square^{-1}. After the slurry coating, the sheet resistance is 100 Ω square^{-1}, this suggests that the super P carbon filler contributes minimally to planar electronic percolation.

For aqueous battery systems, avoiding oxygen and hydrogen evolution is crucial. TiP_2O_7 with an electrochemical potential of 2.6 V versus Li/Li$^+$ and 0.1 V versus SHE (standard hydrogen electrode), is in the electrolysis free window, but $LiMn_2O_4$ has a significant amount of capacity above 4 V versus Li/Li$^+$ and 1.5 V vs. SHE, which is about 0.2 V above the oxygen evolution voltage [16]. However, $LiMn_2O_4$ has been shown to work well in aqueous batteries [9,10], potentially because of kinetic limitations on oxygen evolution that result from the surface chemistry of this material. Fig. 3a plots a typical charge–discharge curve for the aqueous paper battery. The current density is 2C with respect to the weight of TiP_2O_7. The cell is designed with excess capacity in the $LiMn_2O_4$ in order to protect the cathode from overcharge. In this curve, the battery is shown to deliver a discharge capacity of around 90 mAh g^{-1} with respect to TiP_2O_7 and working voltage of about 1.4 V. The overpotential between the charge and discharge plateaus is less than 0.1 V, which reflects the facile reaction kinetics of both materials and the excellent electronic percolation of the paper based current collectors.

In order to check the rate capability of the aqueous paper battery, it is discharged at different current densities. The discharge

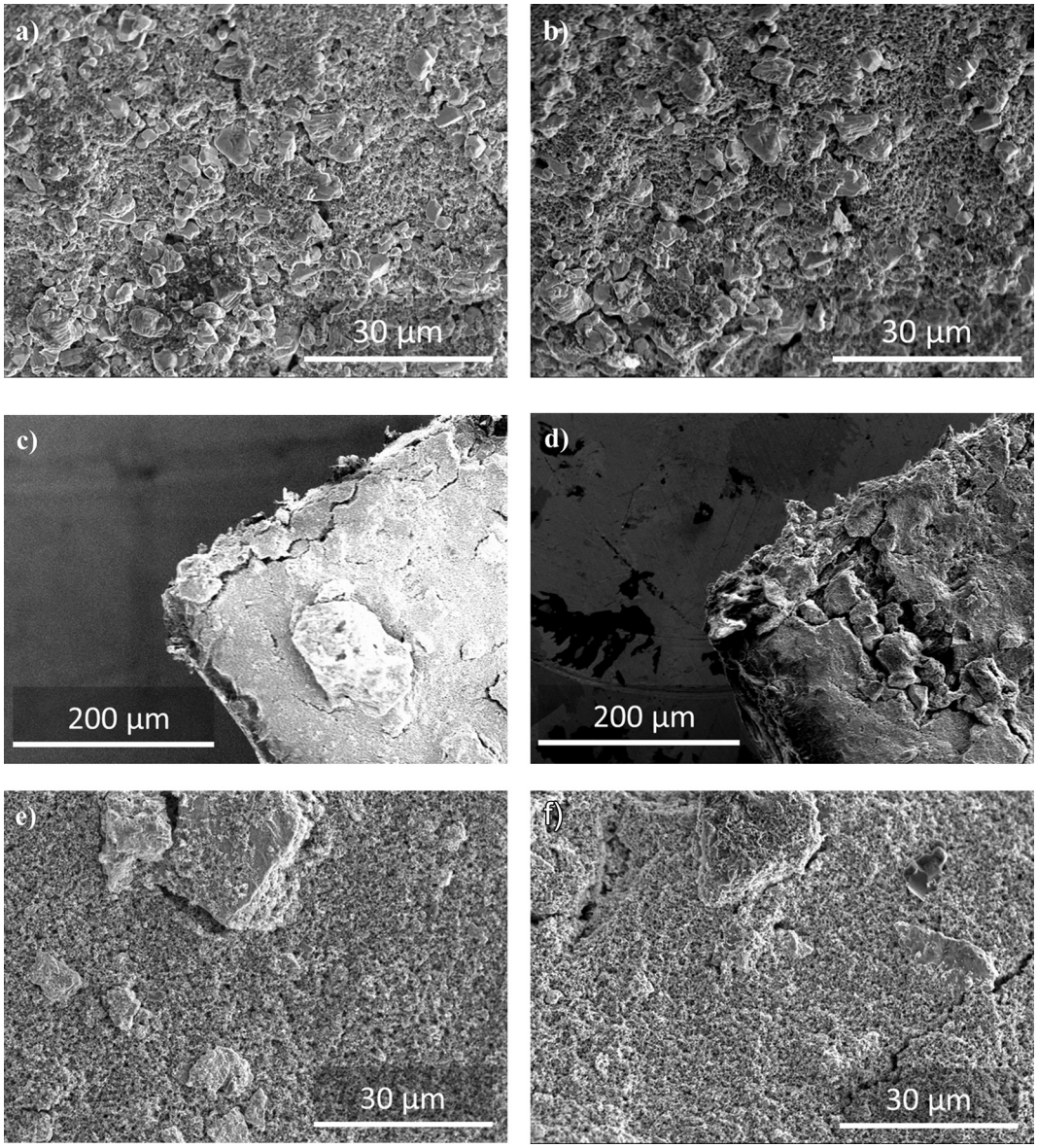

Fig. 4. SEM images of $LiMn_2O_4$ electrodes before (a) and after (b) 10 galvanostatic cycles. Low magnification images of TiP_2O_7 electrodes before (c) and after (d) 10 galvanostatic cycles. High magnification images of TiP_2O_7 electrodes before (e) and after (f) 10 galvanostatic cycles.

curves are shown in Fig. 3b. At 2C, the cell maintains over 90% of its theoretical capacity, and even at 10C it continues to deliver about one third of its theoretical capacity. This slightly outperforms its non-aqueous counterpart in the $LiMn_2O_4$–$Li_4Ti_5O_{12}$ system [6]. However, the results are difficult to directly compare given the different chemistries and particle size distributions in the two works. The rate performance of aqueous paper battery was also compared with other types of aqueous batteries in a Ragone plot shown in Fig. 3c. The aqueous paper battery outperforms other standard aqueous secondary batteries with regards to gravimetric energy and power density. The lithium intercalation system used here has inherently superior specific capacity and the lightweight paper substrate reduces the mass penalty associated with inactive system components: in order to deliver a same capacity with TiP_2O_7 electrode, the weight of paper current collector used is calculated to be 18.4 mg mAh^{-1}, while 37.4 mg mAh^{-1} of stainless steel foil is needed.

The cycle life of the complete cell was tested at 2C for over 100 cycles, and it is shown in Fig. 3d. After 100 cycles, the cell maintains approximately one third of its original capacity. This cannot be compared directly to most non-aqueous Li-ion battery systems since nearly no passivation occurs in aqueous Li-ion battery to alleviate the side reactions [16], but when compared with some aqueous lithium ion batteries, this cell performs reasonably well [9,17]. Another report utilizing $LiMn_2O_4$–TiP_2O_7 on metallic current collectors in aqueous electrolyte [9] observed a two thirds reduction in capacity after only 25 cycles.

To investigate the mechanism for capacity fade, SEM images of $LiMn_2O_4$ and TiP_2O_7 electrodes were taken, at the same location, before and after 10 cycles of charge and discharge at 1C. As shown in Fig. 4a and b, the morphology of the $LiMn_2O_4$ electrode is relatively stable over the 10 cycles. However, the TiP_2O_7 electrode exhibits tremendous morphological change in the same period. Fig. 4c and d demonstrates that an ~100 μm particle was reduced to form several much smaller particles after cycling. Fig. 4e and f reveals the complete disappearance of several 5–10 μm particles and an ~30% reduction in the size of a 30 μm particle. These observations are indicative of TiP_2O_7 dissolution during cycling. This process leads to the observed capacity fade, and the volume of dissolved TiP_2O_7 is qualitatively comparable to the amount of capacity fade over 10 cycles, ~40%. The improvement in cycling life compared to an earlier study [9] might be explained by the improved chemical stability of the surface imparted by the additional carbon coating TiP_2O_7 applied here.

4. Conclusion

This work demonstrated an aqueous paper battery based on an electrochemical couple between $LiMn_2O_4$ and carbon coated TiP_2O_7 electrodes on carbon nanotube coated paper current collectors. SWCNT coating significantly reduces the sheet resistance of the paper and provides a robust framework for electrode penetration. The system exhibits enhanced rate capability relative to comparable non-aqueous systems and improved cycle life relative to similar systems fabricated on metal current collectors. The mechanism for capacity fade is associated with TiP_2O_7 dissolution.

Acknowledgments

This material is based upon work supported by the National Science Foundation (') under award number DMI-0749028. We appreciate the support of Nano-CEMMS in facilitating this research.

References

[1] I.E.S. Edwards, The Early Dynastic Period in Egypt, Univ. Press, Cambridge, 1964.
[2] G. Rao, MRS Bull. 30 (2005) 418.
[3] N. Kaihovirta, C. Wikman, T. Makela, C. Wilen, R. Osterbacka, Adv. Mater. 21 (2009) 2520.
[4] F. Eder, H. Klauk, M. Halik, U. Zschieschang, G. Schmid, C. Dehm, Appl. Phys. Lett. 84 (2004) 2673.
[5] D. Hecht, L. Hu, G. Gruner, Curr. Appl. Phys. 7 (2007) 60.
[6] L. Hu, J. Choi, Y. Yang, S. Jeong, F. La Mantia, L. Cui, Y. Cui, Proc. Natl. Acad. Sci. U. S. A. 106 (2009) 21490.
[7] M. Koo, K. Park, S. Lee, M. Suh, D. Jeon, J. Choi, K. Kang, K. Lee, Nano Lett. 12 (2012) 4810.
[8] W. Li, J. Dahn, D. Wainwright, Science 264 (1994) 1115.
[9] H. Wang, K. Huang, Y. Zeng, S. Yang, L. Chen, Electrochim. Acta 52 (2007) 3280.
[10] J. Luo, Y. Xia, Adv. Funct. Mater. 17 (2007) 3877.
[11] A. Russo, B. Ahn, J. Adams, E. Duoss, J. Bernhard, J. Lewis, Adv. Mater. 23 (2011) 3426.
[12] M. Jo, S. Jeong, J. Cho, Electrochem. Commun. 12 (2010) 992.
[13] L. Shen, H. Li, E. Uchaker, X. Zhang, G. Cao, Nano Lett. 12 (2012) 5673.
[14] Y. Wang, Y. Wang, E. Hosono, K. Wang, H. Zhou, Angew. Chem. Int. Ed. 47 (2008) 7461.
[15] S. Patoux, C. Masquelier, Chem. Mater. 14 (2002) 5057.
[16] J. Luo, W. Cui, P. He, Y. Xia, Nat. Chem. 2 (2010) 760.
[17] G. Wang, L. Fu, N. Zhao, L. Yang, Y. Wu, H. Wu, Angew. Chem. Int. Ed. 46 (2007) 295.